Level structure of the odd mass Pr isotopes. III. Levels of ^{147}Pr$_{88}$ populated in the beta decay of 56-s ^{147}Ce

P. F. Mantica

Department of Chemistry and Biochemistry, University of Maryland, College Park, Maryland 20742
and UNISOR, Oak Ridge Institute for Science and Education, Oak Ridge, Tennessee 37831

J. D. Robertson,* E. M. Baum,* and W. B. Walters

Department of Chemistry and Biochemistry, University of Maryland, College Park, Maryland 20742

The structure of ^{147}Pr has been investigated by performing measurements of γ-ray and conversion-electron singles and $\gamma\gamma$ coincidence spectra of mass separated sources of 56-s ^{147}Ce. The proposed level scheme extends the known structure of ^{147}Pr to an energy of 2.2 MeV and includes several levels below 1.2 MeV that have not been identified in previous decay studies of ^{147}Ce. Measurement of the conversion coefficients for several transitions has led to the assignment of negative parity to the levels at 362, 452, 467, and 608 keV in ^{147}Pr, which show properties similar to low-energy negative-parity states identified in ^{145}Pr$_{86}$, ^{145}La$_{88}$, and ^{149}Pm$_{88}$. The presence of low-energy negative-parity states suggests that configurations having significantly different deformation, related to the highly deformed region above $N = 90$ and/or to the reflection asymmetric region identified around ^{145}Ba, may manifest themselves at low energy in these nuclides.

PACS number(s): 23.20.Lv, 27.60.+j, 21.60.Ev, 23.40.Hc

I. INTRODUCTION

The neutron-rich praseodymium isotopes with $N > 82$ have proton number (59) and neutron numbers (82–88) such that they are influenced both by the presence of strong deformation observed for nuclides with $N \geq 90$ and by reflection asymmetric shapes found near ^{144}Ba$_{88}$. As a consequence of the $Z = 64$ subshell, the transition from spherical to deformed shape occurs very rapidly in the even-A $_{60}$Nd, $_{62}$Sm, and $_{64}$Gd isotopes at $N = 90$, where the $E(4^+)/E(2^+)$ ratio is observed to increase from ~ 2.3 to ~ 3.0 with the addition of two neutrons to the $N = 88$ isotones ^{148}Nd, ^{150}Sm, and ^{152}Gd. Spherical-deformed shape coexistence [1–3] has also been proposed for the Sm and Gd isotopes that reside on either side of the $N = 90$ isotone line. However, an alternate interpretation [4] suggests that the proposed deformed bands can be explained using a simple pairing-plus-quadrupole description.

The experimental identification of strong octupole correlations [5–9] in nuclei around ^{145}Ba as predicted by Leander et al. [10] extends, in even-A nuclei, from ^{144}Ba to ^{150}Sm. The signature of these correlations is the presence of both low-energy negative-parity states, such as the 1^- state in ^{146}Ba, which lies at 739 keV and strong $E1$ transitions down an yrast sequence including both positive- and negative-parity states in the spin range from 4 to 11. Although there was little strong experimental

evidence for octupole structures marked by parity doublets at low energy in the odd-A Ba and Ce isotopes in this region [11,12], the structure of these weakly deformed nuclides is not readily accounted for by considering only quadrupole deformation.

In two previous papers designated I and II, structures for the odd-A isotopes ^{143}Pr$_{84}$ and ^{145}Pr$_{86}$, respectively, have been reported [13,14]. The low-energy positive-parity levels were found to be reproduced well in the framework of the particle truncated quadrupole model (PTQM), in which the Pr nuclides were described as proton quasiparticles coupled to the appropriate Ce even-even core. The calculations did require the introduction of the $d_{3/2}$ proton orbital, which lies above the $Z = 64$ subshell closure, to account for the low-energy $3/2^+$ levels present in ^{145}Pr. These calculations are readily comparable to interacting boson-fermion calculations that provide a good description of the isotonic Eu nuclides [15]. The appearance of negative-parity levels in ^{145}Pr at relatively low excitation energies, specifically, the $3/2^-$ and $5/2^-$ levels at 787 and 1210 keV, respectively, is much more difficult to describe theoretically both for the Pr nuclides and for the Pm nuclides [16].

We have undertaken the study of the levels of ^{147}Pr populated by the β^- decay of 56-s ^{147}Ce to investigate further the approach to deformation in the odd-A Pr isotopes at the $N = 88$ transition point. Previous decay studies [17,18] of ^{147}Ce had resulted in the identification of levels in ^{147}Pr at 2.7, 93, 292, 362, 467, 803, and 1194 keV. The work by Schussler et al. [17] also included several additional levels below 1.0 MeV, although placement of these levels appeared to be solely on the basis of energy summing with the ground state and the 2.7-keV

*Present address: Department of Chemistry, University of Kentucky, Lexington, KY 40506.

level. Spin and parity of $5/2^+$ and $7/2^+$ had been proposed for the ground state [19] and first excited state of ^{147}Pr, respectively, corresponding to the occupation of the proton $d_{5/2}$ and $g_{7/2}$ orbitals. The level at 93 keV was observed to have a half-life of 12 ns.

In a previous publication, we have reported [20] initial results for the level scheme of ^{147}Pr populated by the decay of ^{147}Ce. These included the support for placement of several additional levels below 750 keV, including levels at 28, 246, 385, 471, and 638 keV. In this paper, we present a complete report of our study of the decay of ^{147}Ce, which has included not only γ-ray singles and $\gamma\gamma$ coincidence measurements, but also low-energy γ-ray and conversion-electron singles measurements.

II. EXPERIMENTAL PROCEDURES

The investigation of the β^- decay of ^{147}Ce was performed at the TRISTAN on-line mass separator facility [21] at the High Flux Beam Reactor at Brookhaven National Laboratory where radioactive nuclides were produced by the neutron induced fission of a ^{235}UC target. Both the high-temperature plasma and surface ionization sources [22,23] were used to ionize the fission products to a single positive charge, after which the products were extracted out of the ion source and mass separated. Three separate experiments were carried out for these measurements.

In the initial measurements of γ-ray singles and $\gamma\gamma$ coincidence spectra, the separated $A=147$ activity was deposited for 75 s onto a Mylar tape at the collection station of a moving tape system. The beam was then deflected from the tape for 25 s, after which the activity was moved to the counting station. During this 25-s deflection period, the parent 4.1-s ^{147}La was allowed to decay. The counting station consisted of two Ge(Li) detectors and a Ge detector, each having an energy resolution better than 2.0 keV at 1.3 MeV. γ-ray singles data were collected up to 2.0 MeV in each of the detectors, and twofold coincidence data were collected for each two-detector combination. Time-dependent γ-ray singles spectra were also collected in ten 10-s time intervals using the Ge detector.

In order to obtain more information on low-energy transitions in the decay of ^{147}Ce, a second measurement was completed using two large volume cylindrical Ge detectors and a high-resolution thin planar Ge detector. Separated $A=147$ activity was deposited onto a Mylar tape for 40 s, after which the activity was moved midway between the collecting and counting stations for 40 s before being transported to the counting station. γ-ray singles spectra were recorded up to energies of 400 keV for the planar detector, and to energies of 1.6 and 3.0 MeV for the two Ge detectors. Time-dependent γ-ray singles data were collected in four 10-s time intervals using the Ge detector having the higher gain setting. As before, twofold $\gamma\gamma$ coincidence data were collected for each two-detector combination.

A measurement of γ-ray and conversion-electron singles spectra was also made for the decay of ^{147}Ce. The $A=147$ activity was deposited onto a Mylar tape for 50

s, and then moved to the counting station after a beam deflect period of 25 s. The counting station consisted of a Si(Li) electron detector [11], which had an active area of 200 mm^2 and a depletion depth of 3 mm, and a Ge detector. The energy resolution was better than 2.1 and 2.3 keV at 1.0 MeV for the Ge and electron detector, respectively. A singles spectrum was collected from the Si(Li) detector up to an energy of 1.3 MeV. Two separate amplifiers were used to collect singles spectra from the Ge detector to energies of 2.0 and 4.0 MeV.

III. EXPERIMENTAL RESULTS

A proposed level scheme for the β^- decay of 56-s ^{147}Ce to levels in ^{147}Pr is shown in Fig. 1. The γ rays assigned to the decay of ^{147}Ce and their placement in the level scheme for ^{147}Pr and listed in material deposited with the Physics Auxiliary Publication Service, as is a list of the observed coincidences [24]. The experimental conversion coefficients for several of the more intense transitions in the decay ^{147}Ce are listed in Table I. Portions of the electron and γ-ray spectrum are shown in Fig. 2 that support the conversion coefficients listed in Table I.

The β feeding to levels in ^{147}Pr is given in Fig. 1, where only branches exhibiting greater than 2% of the total β intensity from the parent ^{147}Ce are shown. It is important to note that the $\log f_0 t$ values given in Fig. 1 should be regarded as lower limits, as approximately 85 units of γ-ray intensity remains unplaced in the proposed level scheme. The values for the β feeding shown in Fig. 1 are derived from a measurement in which a saturated source at equilibrium of ^{147}Ce and ^{147}Pr is prepared and a spectrum taken at equilibrium. The total amount of ^{147}Ce is derived from an absolute intensity value of 24% for the 315-keV transition in ^{147}Nd populated in the decay of 13-min ^{147}Pr. This value for the absolute intensity of the 315-keV transition was not adopted in the most recent Nuclear Data Sheets for the $A=147$ mass chain [25], where, instead, a value of 12.60% has been chosen. As the value for the absolute intensity of this γ ray is used to determine the total number of parent ^{147}Ce nuclides, the 12.60% value requires approximately twice as many parent atoms to be present, and hence a very large ground-to-ground β branching in ^{147}Ce decay. Arguments in favor of adopting the value of 24% for the absolute intensity of the 315-keV transition in ^{147}Nd were discussed by Robertson et al. [11] for β branching systematics of the La isotopes in these mass chains. Using the value of 12.60% for the absolute intensity of the 315-keV transition in ^{147}Nd would require that nearly 50% of the total β feeding from the decay of ^{147}Ce populated the lowest three positive-parity states in ^{147}Pr. This is contrary to the β decay systematics of the lighter Pr nuclides, where only 7.0% of the β intensity from the decay of ^{145}Ce directly populates any of the positive parity levels below 800 keV in ^{145}Pr [14]. Instead, it appears as if the β decays from both ^{145}Ce and ^{147}Ce preferentially populate levels having negative parity.

Several γ rays assigned to the decay of ^{147}Ce have multiple placements. The 359-keV γ ray is placed as depopulating the 452-keV state as this transition is observed to
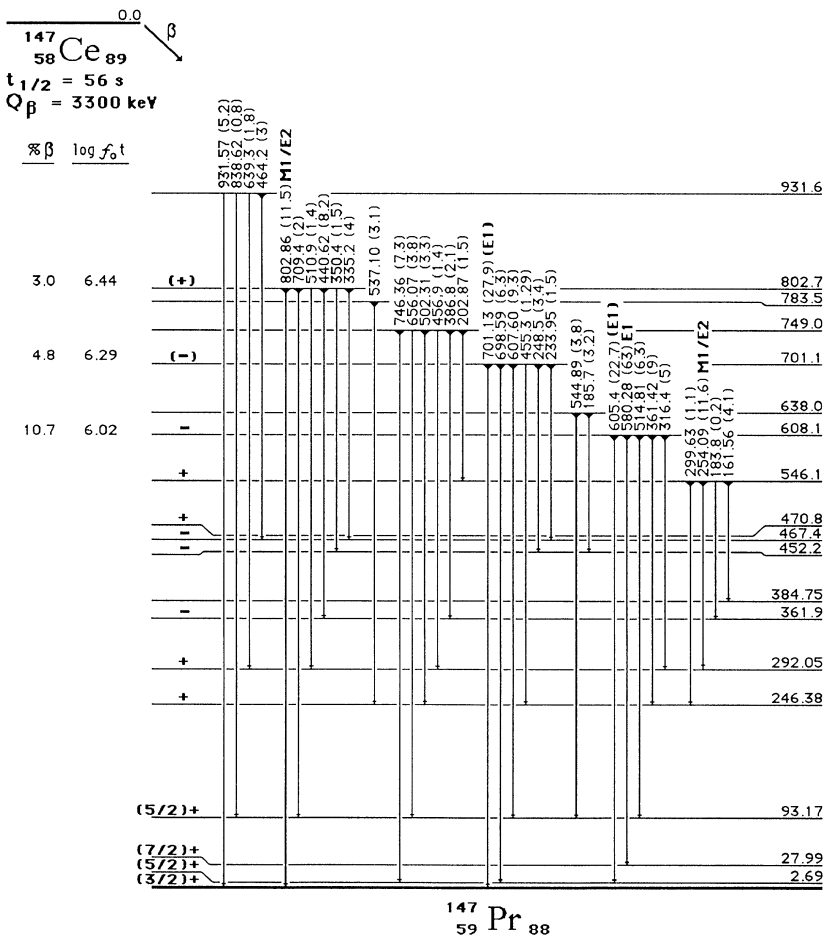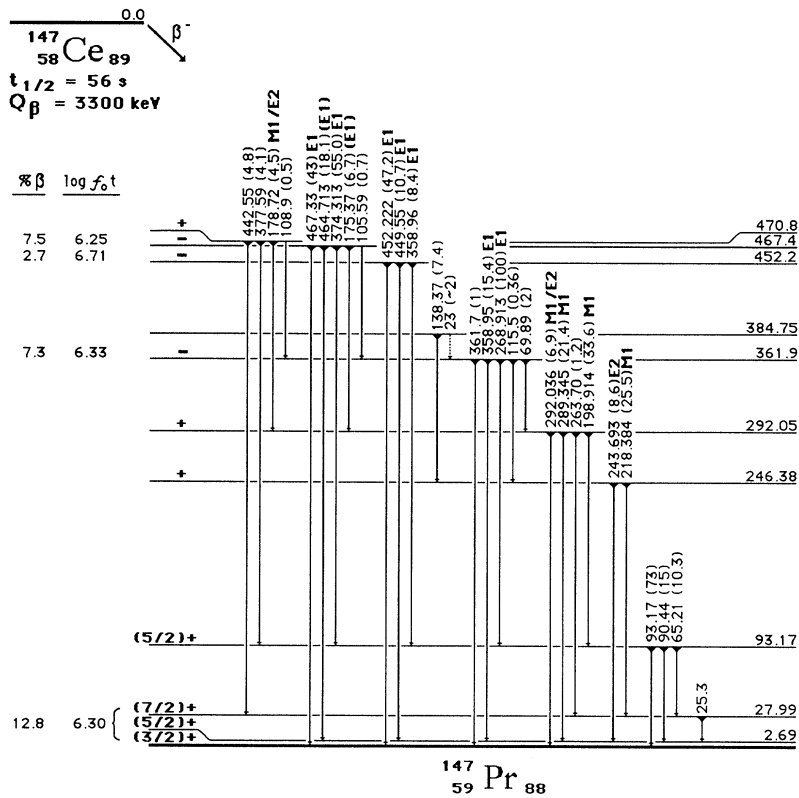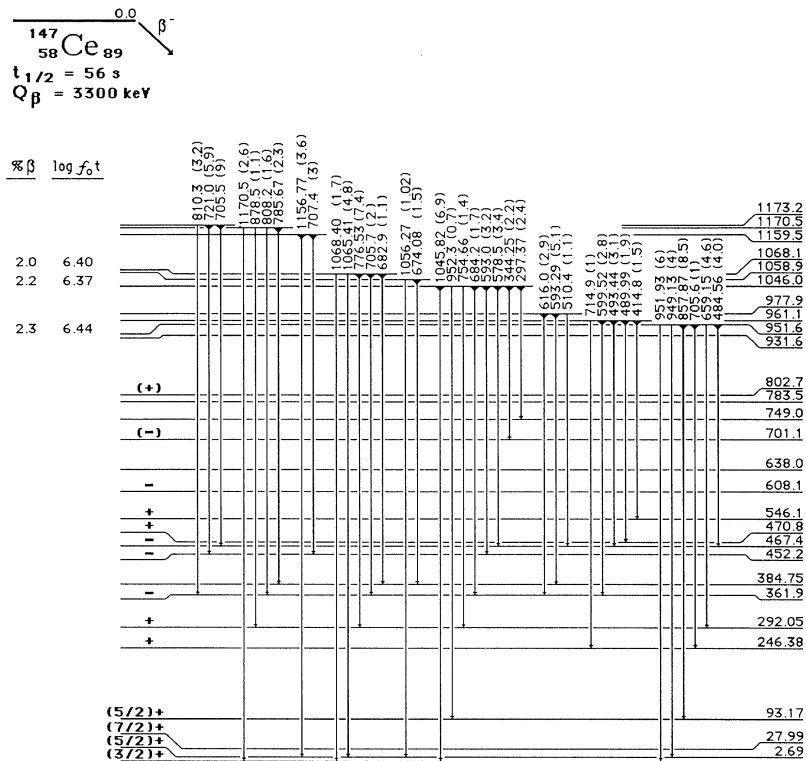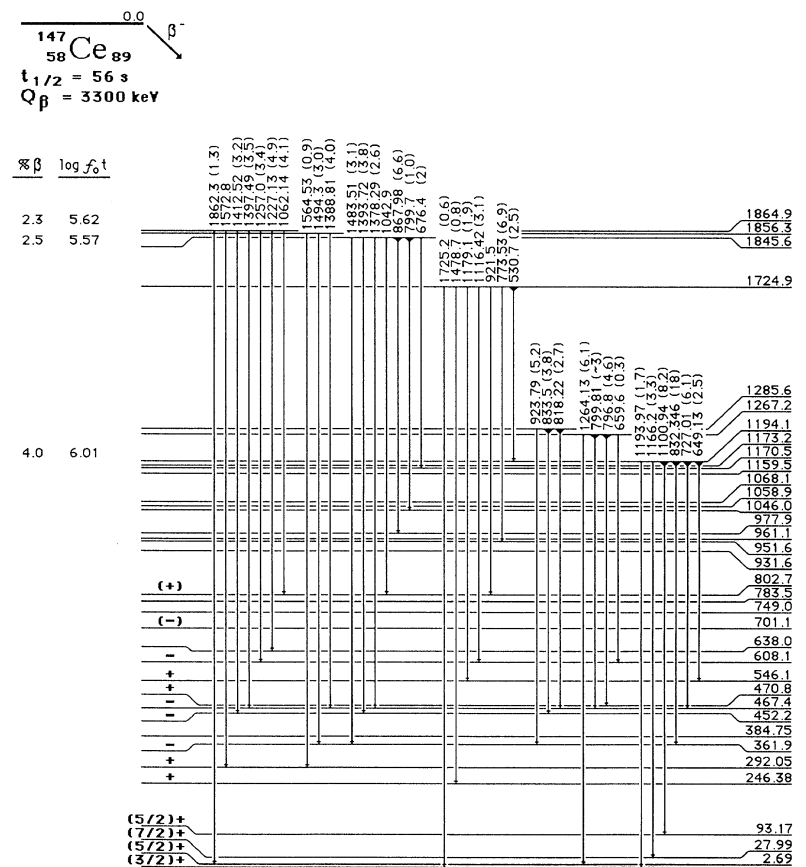
FIG. 1. (a) Proposed level scheme for ^{147}Pr from 0 to 500 keV. The marked transitions are those for which a gated coincidence spectrum was obtained. (b) Proposed level scheme for ^{147}Pr from 0 to 940 keV. (c) Proposed level scheme for ^{147}Pr from 0 to 1200 keV. (d) Proposed level scheme for ^{147}Pr from 0 to 1900 keV. (e) Proposed level scheme for ^{147}Pr from 0 to 2200 keV.

$^{147}_{58}Ce_{89}$ 0.0 β^-

$t_{1/2} = 56$ s

$Q_\beta = 3300$ keV

%β   log $f_0 t$

2.0   6.40

2.2   6.37

2.3   6.44

(+)

(−)

−

+

+

−

−

−

+

+

(5/2)+   93.17

(7/2)+   27.99

(5/2)+

(3/2)+   2.69

Levels: 1173.2, 1170.5, 1159.5, 1068.1, 1058.9, 1046.0, 977.9, 961.1, 951.6, 931.6, 802.7, 783.5, 749.0, 701.1, 638.0, 608.1, 546.1, 470.8, 467.4, 452.2, 384.75, 361.9, 292.05, 246.38, 93.17, 27.99, 2.69

$^{147}_{59}Pr_{88}$

FIG. 1. (Continued).

$^{147}_{58}Ce_{89}$ 0.0 β^-

$t_{1/2} = 56$ s

$Q_\beta = 3300$ keV

%β   log $f_0 t$

2.3   5.62

2.5   5.57

4.0   6.01

(+)

(−)

−

+

+

−

−

−

+

+

(5/2)+   93.17

(7/2)+   27.99

(5/2)+

(3/2)+   2.69

Levels: 1864.9, 1856.3, 1845.6, 1724.9, 1285.6, 1267.2, 1194.1, 1173.2, 1170.5, 1159.5, 1068.1, 1058.9, 1046.0, 977.9, 961.1, 951.6, 931.6, 802.7, 783.5, 749.0, 701.1, 638.0, 608.1, 546.1, 470.8, 467.4, 452.2, 384.75, 361.9, 292.05, 246.38, 93.17, 27.99, 2.69

$^{147}_{59}Pr_{88}$

$^{147}_{58}\text{Ce}_{89}$ 0.0 β^-

$t_{1/2} = 56$ s

$Q_\beta = 3300$ keV

%β   log $f_0 t$

5.8   5.10

2249.5
2183.0
2135.5
2060.8
1944.0
1864.9
1856.3
1845.6
1724.9
1285.6
1267.2
1194.1
1173.2
1170.5
1159.5
1068.1
1058.9
1046.0
977.9
961.1
951.6
931.6
802.7
783.5
749.0
701.1
638.0
608.1
546.1
470.8
467.4
452.2
384.75
361.9
292.05
246.38
93.17
27.99
2.69

(+)
(−)
−
+
+
−
−
−
+
+

(5/2)+
(7/2)+
(5/2)+
(3/2)+

$^{147}_{59}\text{Pr}_{88}$

FIG. 1. (Continued).

be in coincidence with the three transitions that deexcite the level at 93 keV. The placement of a 359-keV transition from the level at 362 keV is supported by the appearance of the 387-, 441-, and 832-keV γ rays in the gated spectrum for the 359-keV γ ray.

Most of the intensity of the 361-keV γ-ray doublet is assigned to the transition out of the level at 608 keV, supported by the observed 361-218 and 361-244 coincidence relationships. Also present in the 361-keV gated spectrum was a small peak corresponding to the 832-keV γ-ray transition, which is placed as populating the 362-keV state from the level at 1194 keV. This has resulted in the placement of a very weak 361.7-keV transition from the 362-keV level to the ground state.

A similar case holds for the 465-keV doublet, where the major fraction of the intensity has been placed as a 464.7-keV transition out of the level at 467 keV based on the 465-706 and 465-727 coincidence relationships. However, the observed 465-467 coincidence relationship warranted the placement of the 464.2-keV transition from the level at 932 keV to the 467-keV state.

The lower-energy member of the 510-keV γ-ray doublet has been placed as depopulating the level at 978 keV, as this transition was observed in the gated spectra for the 374- and 467-keV transitions. The higher-energy member of the doublet is placed as populating the 292-keV state based on the 199-510 coincidence relationship.

The 593-keV doublet consists of the 593.0-keV transition placed in the proposed level scheme as populating the level at 452 keV based on the 593-452 coincidence relationship, and the 593.3-keV transition, which feeds the level at 385 keV based on the observation of the 138-keV γ-ray peak in the gated spectrum of the 593-keV transition.

Most of the γ-ray intensity of the doublet at 659 keV is placed as a 659.2-keV transition from the level at 952 keV to the 292-keV state based on the appearance of a γ-ray peak at 659 keV in the gated spectra of the 199-, 289-, and 292-keV transitions. A 659.6-keV transition is also placed between the levels at 1267 and 608 keV based on the 605-659 coincidence relationship. The majority of the intensity of the doublet at 800 keV is proposed to deexcite the level at 1267 keV based on the observed 800-374 and 800-467 coincidences. The additional placement, as populating the state at 1046 keV, is a result of the appearance of a peak corresponding to the 800-keV γ ray in the gated spectrum for the 1046-keV transition.

The γ ray appearing at 952 keV in the singles spectrum

TABLE I. Experimental conversion coefficients for transitions following the β decay of ^{147}Ce.

Transition energy (keV)	10^3 conversion coefficient[a]		Theoretical $10^3 K$ conversion[b]		
			$M1$	$E2$	$E1$
162	$-K$	457(18)	291	277	57.3
175	$-K$	87(8)	236	217	46.5
179	$-K$	317(13)	221	202	43.7
199	$-K$	175(5)	166	144	32.9
	$-L$	35(5)			
218	$-K$	175(4)	129	108	25.7
234	$-K$	97(27)	107	86.4	21.3
244	$-K$	77(4)	95.8	75.6	19.1
254	$-K$	78(3)	86.1	66.6	17.1
269	$-K$	14.0(4)	74.0	55.7	14.7
289	$-K$	74(2)	61.3	44.7	12.2
292	$-K$	52.2(4)	59.6	43.3	11.9
359/361[c]	$-K$	7.7(11)	34.8	23.5	7.11
374	$-K$	6.1(6)	31.3	20.9	6.43
450/452[c]	$-K$	3.4(5)	19.3	12.4	4.10
464	$-K$	6.2(15)	18.1	11.5	3.86
467	$-K$	4.7(7)	17.8	11.3	3.81
575/580[c]	$-K$	2.7(4)	10.3	6.46	2.34
800/802[c]	$-K$	9(2)	4.69	2.97	1.19

[a]Conversion coefficients normalized to the 269-keV transition K-conversion coefficient theoretical $E1$ value of 14.7×10^{-3} from Rösel et al. [26]. The number(s) in parentheses is the error in the last digit(s) of the value for the experimental conversion coefficient.

[b]Calculated from Rösel et al. [26].

[c] The transition is resolved in the γ-ray singles spectrum, but not in the conversion-electron singles spectrum. The conversion coefficient calculated is for the total γ-ray intensity and total conversion-electron intensity observed for the unresolved multiplet.

is also proposed to be a doublet, where a majority of the intensity is placed as a ground-state transition from the level at 952 keV, and the remaining intensity as populating the level at 93 keV, based on the observed 952-93 coincidence relationship.

A study of the coincidence spectra relating to the γ rays observed in the singles spectrum at 706 and 709 keV reveals several complicated relationships, which has resulted in multiple assignments for these γ rays. The 705.5-keV member of a triplet of γ rays that appears at 706 keV in the singles spectrum is placed as populating the level at 467 keV based on the 374-706, 465-706, and 467-706 coincidence relationships. A very weak transition, corresponding to a transition energy of 705.7 keV, is placed between the levels at 1068 and 362 keV based on the observed 269-706 coincidence relationship. The third member of the triplet has been assigned an energy of 705.6 keV and is placed as depopulating the level at 952 keV based on the 706-218 coincidence relationship. The γ ray proposed at 707.4 keV can be accounted for in the gated coincidence spectrum for the 452-keV transition, where a peak corresponding to a γ-ray transition of 707 keV is observed, resulting in the placement of a level at 1159 keV. For the transition observed in the singles spectrum at 709 keV, only a fraction of the observed intensity can be assigned to the transition from the 803-keV level to the level at 93 keV based on the observed intensities in the gated spectrum for the 93-keV transition. The

remaining intensity remains unplaced in the level scheme proposed here; however, it is interesting to note that there is a distinct 1157-709 coincidence relationship supporting placement of the remaining intensity of the 709-keV transition as feeding the level proposed at 1159 keV. This placement would result in a level at 1869 keV in the level scheme for ^{147}Pr. As we have found no other support for the placement of a level at 1869 keV, it is not included in the present level scheme.

Of the new levels proposed for the level scheme of ^{147}Pr, many are supported by our $\gamma\gamma$ coincidence measurements. The level at 28 keV is supported by the observed coincidence between the 25.3-keV transition and transitions from the previously identified levels at 93 and 292 keV. No intensity value is reported for the 25.3-keV transition as we were unable to reproduce the low-energy efficiency response for the planar detector to any degree of satisfaction using a ^{154,155}Eu, ^{125}Sb mixed calibration source.

The 25.3-keV gate was also instrumental in the placement of the level at 246 keV, as the 218-keV transition is clearly seen in the coincidence gate for this low-energy transition. The 385-keV state has been placed through the observance of a 138-keV transition in both the 218- and 244-keV coincidence gates.

The levels at 452, 471, 608, 638, 701, 749, and 952 keV are placed based on the 359-, 378-, 515-, 545-, 608-, 656-, and 858-keV γ rays, respectively, each of which appear

as peaks in the coincidence spectrum gated on the 93-keV γ-ray transition. Several other coincidence relationships also support these proposed placements.

The level at 546 keV is placed based on the appearance of the 254-keV γ ray in the gated spectrum of each of the γ rays, which depopulated the level at 292 keV. This placement is also supported by the observed coincidence between the 162- and 138-keV γ rays. As the 138-keV γ ray is the sole transition to depopulate the level at 385 keV, the order of the 162-138 decay sequence was determined by the presence of a peak in the 162-keV gated spectrum corresponding to the 269-keV γ-ray transition, which depopulates the level at 362 keV. This suggests that the 162-keV γ ray must deexcite to a level lying above the 362-keV state. Therefore, the proper sequence results with the placement of the 162-keV transition populating the level at 385 keV, and in the placement of a transition between the 385- and 362-keV states; in this case a 23-keV transition, which is tentatively placed in

the level scheme shown in Fig. 1. The total transition intensity of the 23-keV transition is found from the relative peak areas of the 138- and 269-keV peaks in the 162-keV gate.

The 784-keV state is placed on the observance of a 537-keV γ-ray peak in the gated spectra for the 218- and 244-keV transitions, both of which depopulate the level at 246 keV. The levels at 932, 961, 978, 1046, and 1068 keV are placed on the basis of several coincidence relationships, including the appearance of the 600-, 616-, 684-, and 706-keV γ-ray peaks, respectively, in the gated coincidence spectrum for the 269-keV transition, and the 639-keV peak in the 199-keV gate.

A doublet of levels appears at 1170 and 1173 keV in the level scheme for [147]Pr. The lower member of the doublet is placed based on the 786-138 and 878-199 coincidence relationships. The higher member of the doublet is placed as a result of the coincidences observed between the 706- and 374-keV γ rays and the appearance of the
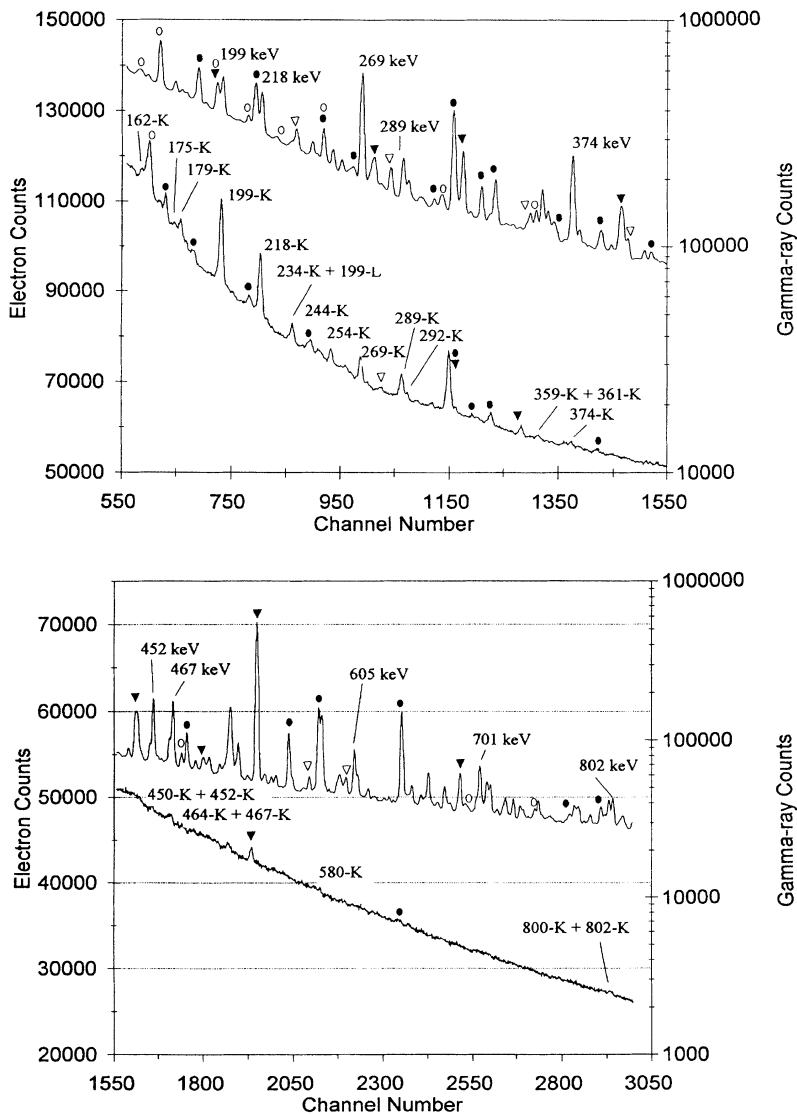

FIG. 2. (a) γ-ray and conversion-electron spectra up to 400 keV for [147]Ce decay. (b) γ-ray and conversion-electron spectra from 400 to 800 keV for [147]Ce decay. (○ — [147]La; ▽ — [147]Ce; ● — [147]Nd; ▼ — [147]Pm.)

359-, 450-, and 452-keV γ rays in the gated spectrum for the 721-keV transition.

The remaining levels shown in Fig. 1 are also supported by from one to several coincidence relationships, which will not be discussed here, but which can be inferred from Fig. 1. Other levels at 1641, 1969, 2121, 2126, 2199, 2242, 2415, and 2442 keV could be proposed as new levels in ^{147}Pr solely on the basis of energy-sum relationships. There are also two doublets at 416 and 419 keV and 732 and 735 keV that are separated by 2.7 keV that might be from levels at 419 and 735 keV that deexcite to the ground and first excited states. As we have no coincidence data to support these placements, they are not shown on the level scheme.

IV. SPIN AND PARITY ASSIGNMENTS

Parity assignments have been made for several of the low-energy levels in ^{147}Pr based on the experimental conversion coefficients which are listed in Table I, and shown graphically in Fig. 3 along with theoretical data from the work of Rösel et al. [26]. On the assumption that the ground-state ^{147}Pr has positive parity, which is supported by both systematics and the β decay [27] to levels in ^{147}Nd, the level at 292 keV must have positive parity, as this level depopulates to the ground state via a 292-keV transition having $M1/E2$ multipolarity. Since the 199- and 289-keV transitions that depopulate this level have $M1+(E2)$ multipolarity, the levels at 2.7 and 93 keV must also have positive parity. The level at 546 keV is proposed to have positive parity, as the 254-keV transition, placed between the 546-keV state and the level at 292 keV, has $M1/E2$ multipolarity. The 179-keV transition, which also populates the level at 292 keV, has $M1/E2$ multipolarity, which results in an assignment of positive parity to the level at 471 keV.

The level at 246 keV is depopulated by a 244-keV γ ray, which is measured to have $E2$ multipolarity, which feeds the level at 2.7 keV. It follows, therefore, that this level have positive parity, and that the 28-keV level also have positive parity, as it is populated by the 218-keV $M1$ transition from the level at 246 keV.

Figure 2 has been specifically included to exhibit the small peaks in the spectrum that are $E1$ transitions. The 362-, 452-, 467-, and 608-keV states are proposed to have negative parity as they deexcite via $E1$ transitions to levels having positive parity. A tentative assignment of negative parity has also been made for the level at 701 keV. Although the 701-keV transition is not observed in the conversion-electron spectrum collected from the decay of ^{147}Ce, its absence from this spectrum is direct evidence for assigning $E1$ multipolarity. As this transition has a large relative intensity (see the intensities given in the level scheme in Fig. 1) as observed in the γ-ray singles spectrum for the decay of ^{147}Ce, its K-conversion peak should have been observed in the electron singles spectrum, if this transition had $M1/E2$ multipolarity. The 605-keV transition is also assigned $E1$ multipolarity based on similar arguments.

Assignment of positive parity has been made for the level at 802 keV based on the determined $M1/E2$ multipolarity for the 802-keV transition. Since the K-conversion line was an unresolved doublet in the conversion-electron spectrum at 802 keV, the positive-parity assignment for the 802-keV level is only made tentatively at this time.

The tentative assignment of the spin sequence of 3/2, 5/2, and 7/2 for the ground state and first two excited states in ^{147}Pr, respectively, is based on the presence of the 25.3-keV transition and absence of a 28-keV transition, and the observation of $l=2$ and 4 transitions in the ^{148}Nd$(t,\alpha)^{147}$Pr proton pickup reaction. The pickup data suggest spin and parity of $7/2^+$ for the 28-keV level and the presence of a γ-ray transition at 25.3, and absence of one at 28-keV indicates a preference for one unit of angular momentum difference between the levels at 2.7 and 28 keV and two units of angular momentum difference between the ground state and the level at 28 keV, i.e., spin and parity of $5/2^+$ for the 2.7-keV level and $3/2^+$ for the ground state. The inversion of the spins of the ground state and level at 28 keV to yield a spin and parity of $7/2^+$ for the ground state is not consistent with the decay of ^{147}Pr to levels of ^{147}Nd, in particular, the rather strong β transition to the $1/2^-$ level at 314.6 keV [25].
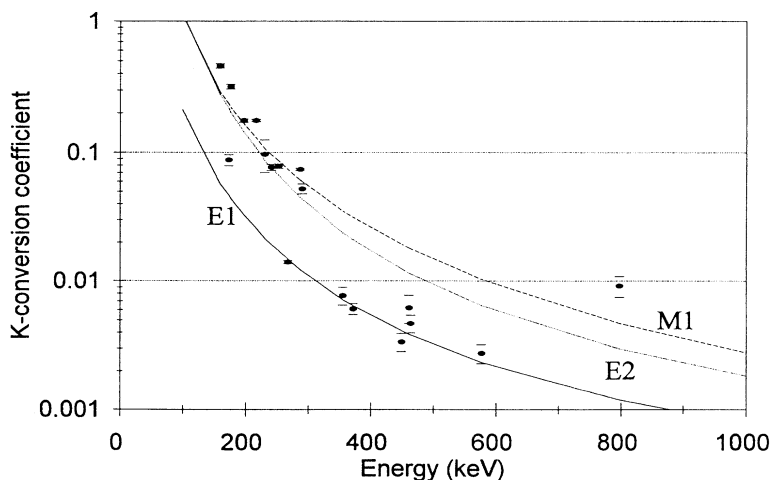

FIG. 3. A plot of $\alpha(K)$ vs γ-ray energy for transitions in ^{147}Pr. The theoretical $E1$, $M1$, and $E2$ curves are taken from Rösel et al. [26].

As the 93-keV level shows transitions of approximately equal intensity to all three members of the ground-state triplet, it is likely a $5/2^+$ level.

V. DISCUSSION

A. Particle-rotor calculations
and positive-parity states in odd-A Pr isotopes

In order to better understand the underlying physics of the low-energy level structure proposed here for ^{147}Pr, we have calculated the structure of the odd-A Pr isotopes above the $N=82$ neutron shell closure in the framework of the particle-plus-triaxial rotor model (PTRM) [28,29]. The calculations involved the diagonalization of the deformed shell-model Hamiltonian to compute single-particle energies and wave functions of a nonaxially symmetric deformed Woods-Saxon potential [31,30].

The deformation parameters $(\beta_2, \beta_4, \gamma)$ used for the Woods-Saxon potential were extracted from total Routhian surface (TRS) calculations [32] for the even-even neighbors of these odd-A Pr isotopes. Shown in Fig. 4 are examples of the surfaces produced from the TRS calculations for the nearest even-even neighbors of ^{145}Pr and ^{147}Pr. From the TRS calculations, it is apparent that the $N=88$ nuclei can be described as axially symmetric ro-

tors, with $\beta_2 \sim 0.17$ and $\gamma=0°$. For the even-even neighbors having two fewer neutrons, however, the quadrupole deformation predicted by the TRS calculations decreases to $\beta_2 \sim 0.12$, and the surfaces begin to show softness in the β degree of freedom toward spherical shape. With the approach to the neutron closed shell at $N=82$, the $N=84$ neighbors of ^{143}Pr are predicted to have deformations where $\beta_2 < 0.10$. Such a low value for the quadrupole deformation in the $N=84$ isotones excludes ^{143}Pr from calculations based on the particle-plus-triaxial rotor framework. But a weak-coupling particle-vibration model has been successful for other $N=84$ isotones, including ^{145}Pm whose structure has recently been described by Glasmacher et al. [33].

The low-energy positive-parity levels calculated using the particle-plus-triaxial rotor code for ^{145,147,149}Pr are shown in Fig. 5, where they are compared with the known experimental levels. In these calculations, the single-particle matrix elements were calculated by selecting all the Nilsson orbitals residing within ± 4 MeV of the Fermi surface. The residual pairing interaction was treated within the BCS approximation, where a standard value of the pairing strength parameter, G, was adopted for each isotope using the prescription of Dudek, Majhofer, and Skalski [34]. The core 2_1^+ energy was estimated by taking the average of the 2_1^+ energies from the
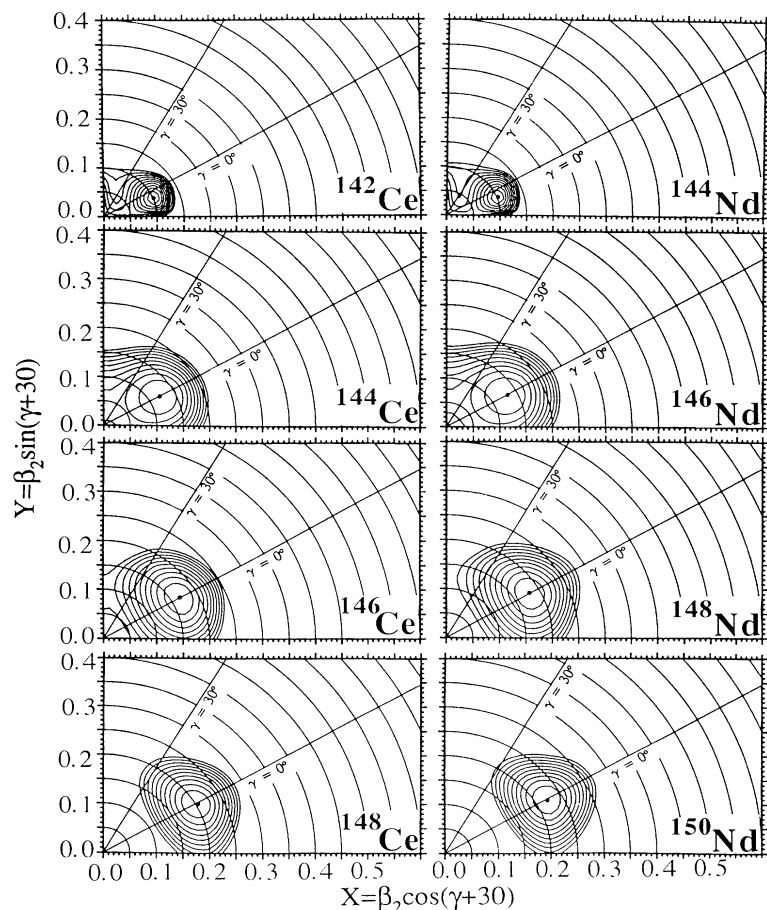

FIG. 4. The TRS plots for the even-even Ce and Nd nuclides with $84 \leq N \leq 90$. The surfaces are calculated at a cranking frequency of $\omega = 0.05$.

neighboring even-even core nuclei. The recoil terms in the particle-plus-triaxial rotor model Hamiltonian were treated as one-body operators as recommended by Semmes [35].

A close comparison of the theoretical level energies to the actual experimental spacings suggests that the PTRM does quite well in predicting the level density at low energy, especially in ^{147}Pr, where the triplet of states found to be within 100 keV of the ground state is well reproduced. However, the PTRM calculations presented here do not reproduce the low-energy levels of ^{145}Pr as well as the PTQM calculations in Ref. [14]. The fact that there is better agreement with the PTRM for the case of ^{147}Pr suggests that the ^{146}Ce core is a better rotor than the ^{144}Ce core.

The predicted level structure for the positive-parity states in ^{147}Pr is shown in Fig. 6. This figure is shown to outline the appropriate band structures, which are predicted to appear at low energy. The magnetic and quadrupole moments are also calculated for each bandhead. Selected results of transition probability calculations are

also given, where the spin g factor has a value 0.70 times the free value. Although definitive spin and parity assignments have not been made to the low-energy levels in ^{147}Pr, we can still qualitatively compare the calculated transition probabilities with those derived experimentally.

From the PTRM calculations for ^{147}Pr, there results an interesting pattern in the decay probabilities between the states that lie lowest in energy. For example, the $7/2^+$ level is predicted to decay most strongly to the two $5/2^+$ levels; the $B(E2)$ branch to the $3/2^+$ state is calculated to be very small. Experimentally, no transition has been observed between the $7/2^+$ state at 28 keV and the $3/2^+$ ground state. Also, the $\Delta I = 1$ transitions from this low-energy $7/2^+$ to the $5/2^+$ states are predicted to have predominantly $E2$ multipolarity. Unfortunately, the low-energy background in the conversion-electron singles spectrum precluded the identification of any low-energy conversion lines, and no multipolarity assignments have been made to these transitions.

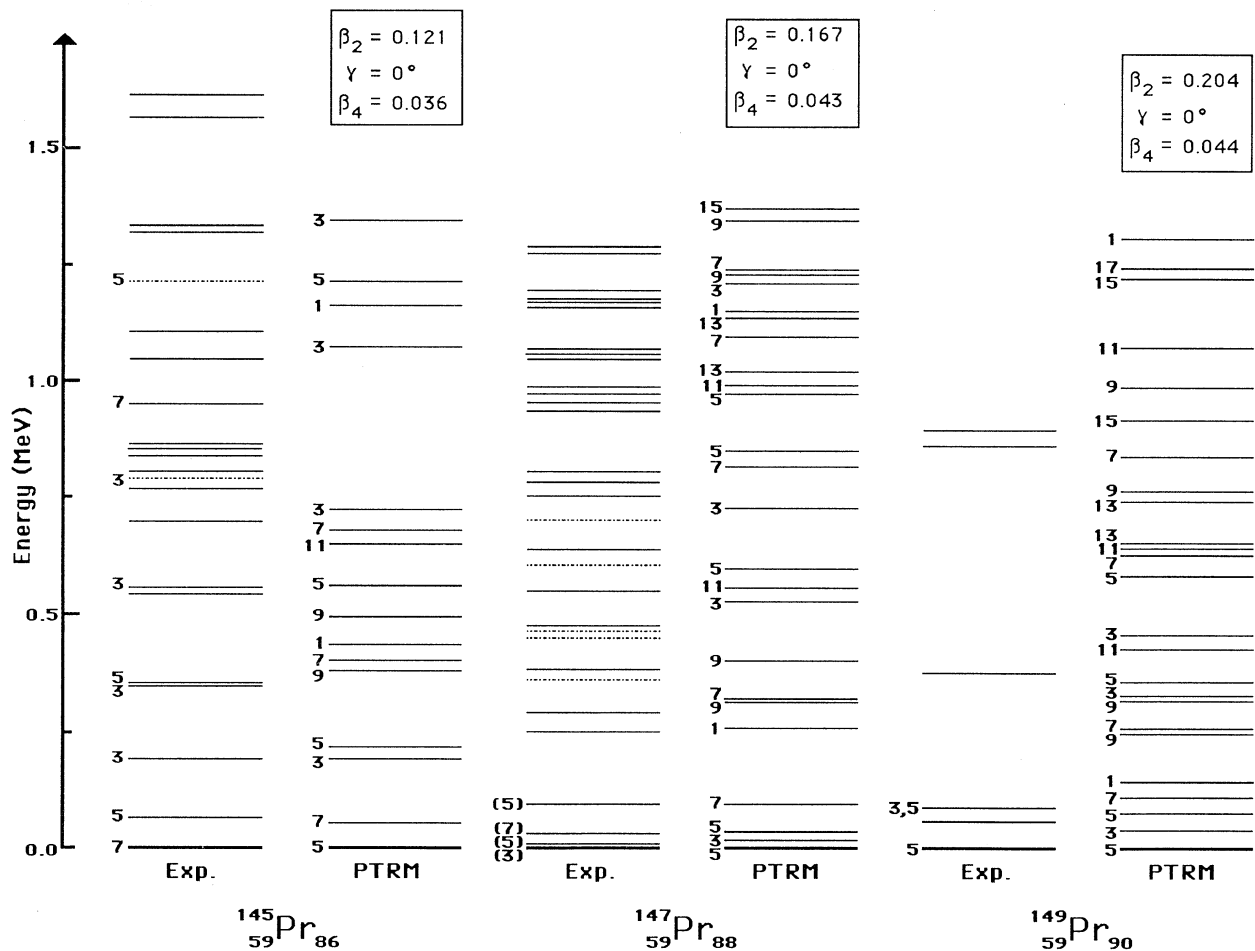Another peculiarity in the calculations is the decay

FIG. 5. Experimental levels in ^{145,147,149}Pr with the positive parity levels calculated from the particle-plus-triaxial rotor model. Deformation parameters were taken from the TRS predictions. Spins are given as 2^*I. Other PTRM parameters are discussed in the text.

branching out of the two, nearly degenerate, $9/2^+$ levels. Very little $B(E2)$ strength is predicted for what should be the stretched $E2$ transitions out of these two levels to the corresponding $5/2^+$ states. The majority of the decay strength instead populates the $7/2^+$ members of each band. A candidate for one of the $9/2^+$ states is the level at 246 keV, which is observed experimentally to be depopulated by γ transitions to the $7/2^+$ state and only one of the $5/2^+$ states.

In all these comparisons, however, it is vitally important to note that the two bands calculated to be lowest in energy are highly mixed. The resulting wave functions for the states assigned to the $[411]\frac{3}{2}$ and $[413]\frac{5}{2}$ bands given in Table II exhibit the extent of the mixing in these two bands. One interesting aspect of the calculations reported here is that there was very little change in the calculated wave functions for these levels in the range where $0.15 \leq \beta_2 \leq 0.18$. That these levels do form the pseudospin doublet $[3\tilde{1}2]\frac{3}{2},\frac{5}{2}$ will only be mentioned at this time, as a detailed investigation into the pseudo SU(3) symmetry limit has not been carried out in this work [36].

B. Low-energy negative-parity levels and octupole deformation in the $N = 88$ isotones

The negative-parity level structures for the odd-A Pr isotopes were also calculated in the framework of the PTRM. Since the particle-plus-triaxial rotor code used here had no provision for mixing of states having opposite parity, separate calculations were performed, using the same deformation parameters, for computing the positive and negative states. The energy spacing between the calculated ground state (having positive parity) and the bandhead of the lowest negative-parity band was determined by calculating the levels of the neighbor nuclides ^{149,151}Pm using the PTRM code. The position of the $11/2^-$ bandhead of the $[505]\frac{11}{2}$ negative-parity band relative to the ground state is known experimentally for both of these nuclides, and this energy difference was used to adjust the position of the calculated $[505]\frac{11}{2}$ bandhead to the lowest-energy positive-parity state. The PTRM calculations for the Pm isotopes were done in the same spirit as the Pr calculations, with the deformation parameters
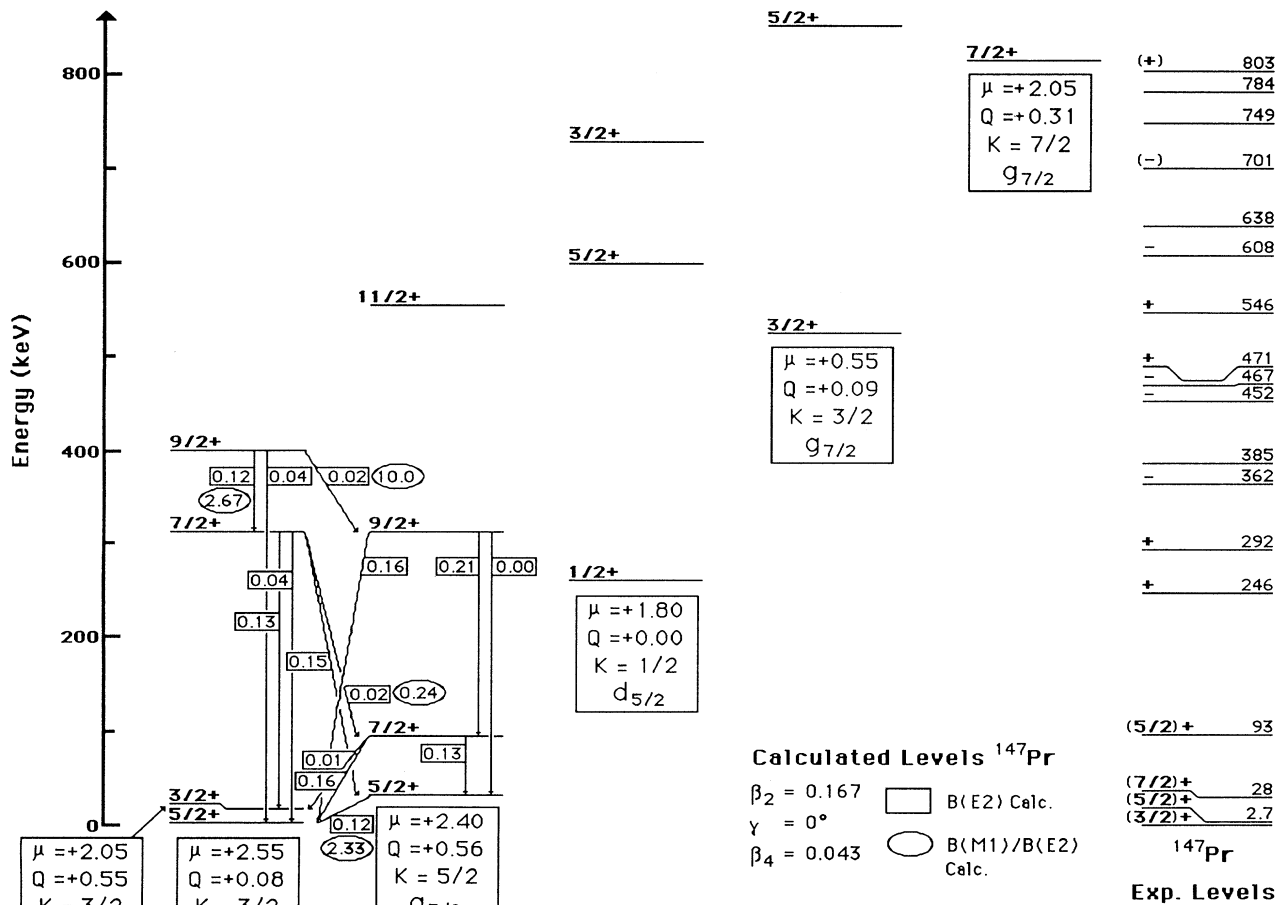

FIG. 6. The calculated band structure of ^{147}Pr. The dominating bands at low energy are based on the $[411]\frac{3}{2}$ and $[413]\frac{5}{2}$ Nilsson orbitals. Predicted $B(E2)$ and $B(M1)/B(E2)$ values are also given for select transitions. The experimental levels in ^{147}Pr are shown to the right.

TABLE II. Wave functions for the $[411]\frac{3}{2}$ and $[413]\frac{5}{2}$ band members calculated for ^{147}Pr.

| J | n | $[431]\frac{1}{2}$ | Mostly $g_{7/2}$ | | | Mostly $d_{5/2}$ | | |
			$[422]\frac{3}{2}$	$[413]\frac{5}{2}$	$[404]\frac{7}{2}$	$[420]\frac{1}{2}$	$[411]\frac{3}{2}$	$[402]\frac{5}{2}$
5/2	(1)		0.145	0.554		0.458	−0.659	0.149
3/2	(1)		−0.059			−0.292	−0.954	
7/2	(2)		0.126	−0.286	−0.102	0.326	0.803	0.371
9/2	(2)	−0.160	−0.306	−0.500	0.227	0.485	−0.526	0.224
11/2	(2)		0.158	−0.327	−0.159	0.330	0.748	0.412
5/2	(2)	0.094	0.294	0.761		−0.310	0.432	−0.196
7/2	(1)	−0.134	0.382	−0.789	−0.316	−0.178	−0.272	−0.073
9/2	(1)		−0.288	−0.639	0.323	−0.372	0.478	−0.187
11/2	(1)	−0.228	0.457	−0.680	−0.341	−0.232	−0.289	−0.125

β_2, β_4, and γ again being derived from TRS calculations.

The results of the normalization of the negative-parity bandhead are shown in Fig. 7, where the predicted negative-parity level structures for ^{145,147,149}Pr are shown, along with the experimental data. The $[505]\frac{1}{2}$ band is predicted to decrease in energy with an increase in the neutron number in these Pr isotopes from $N=86$ to 90. As the $11/2^-$ member of the $[505]\frac{1}{2}$ band has not been identified in any of these Pr isotopes, it is difficult to interpret the predictions from the PTRM.

It is immediately clear, however, that the PTRM calculation does not reproduce the position of the low-spin
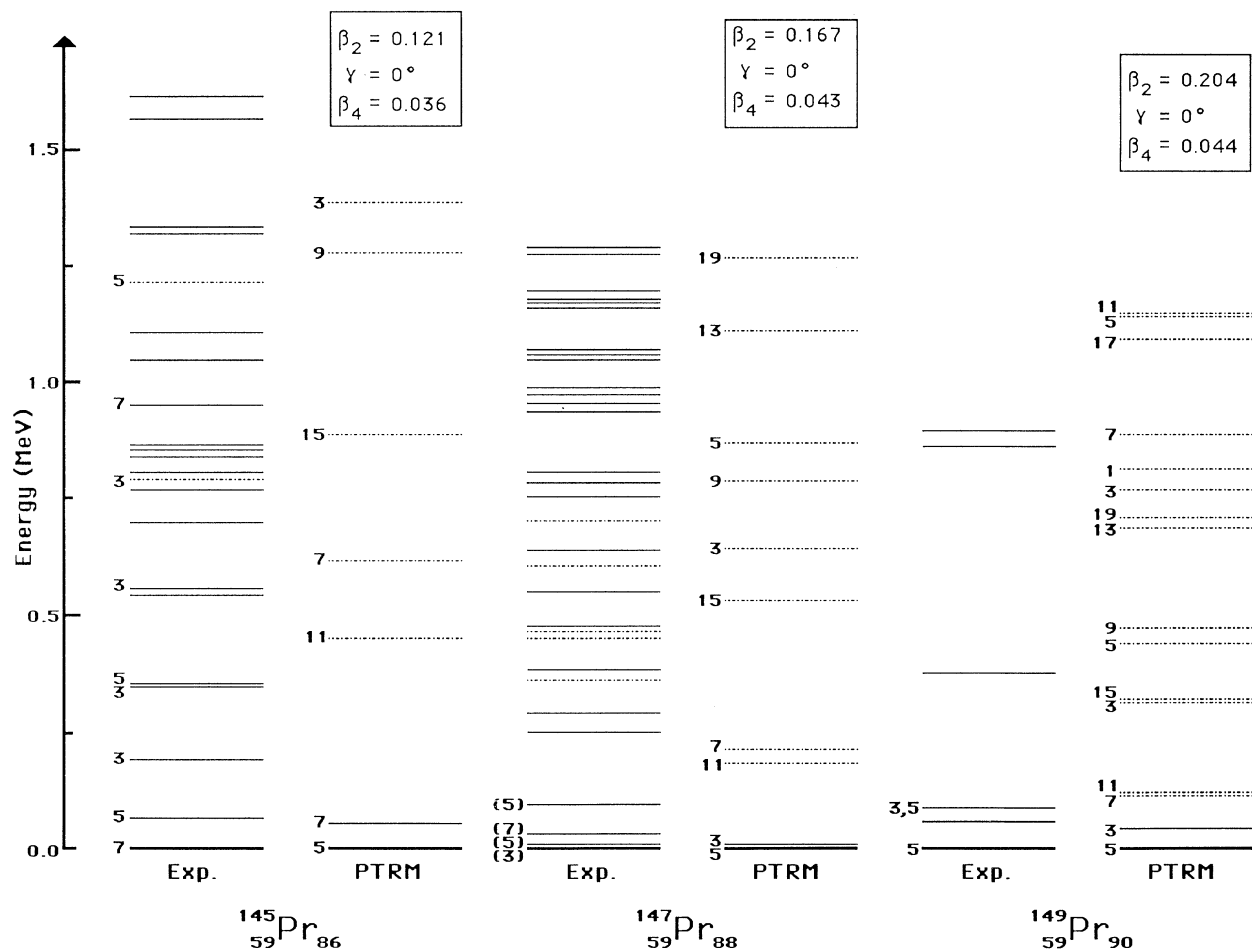

FIG. 7. Experimental levels in ^{145,147,149}Pr with the negative-parity levels calculated from the particle-plus-triaxial rotor model. Deformation and other PTRM parameters used were identical to those used to calculate the positive-parity levels. Spins are given as $2*I$.

negative-parity levels observed in these Pr nuclides. The experimental levels shown in Fig. 7 are again obtained from radioactive decay studies; specifically, the study of β decaying parent nuclides having low spin. (To define a reference frame, low spin is $I \le \frac{9}{2}$.) For [145,147]Pr, where the negative-parity states have been identified from measurements of internal conversion coefficients, there is an apparent excess in low-spin negative-parity states at low energy, above that predicted from the particle-plus-triaxial rotor model. However, no attenuation was used in determining the Coriolis mixing between intrinsic states in the PTRM calculations. The mixing typically is calculated to be too large, especially between states originating from a high-j orbital. Attenuation of this mixing will result in lowering the energy [37] of the non-spin-aligned members of the band build upon the high-j orbital. For the negative-parity levels calculated for the odd-A Pr isotopes, which are members of a band based on the $[505]\frac{1}{2}$ bandhead, a reduction in the Coriolis mixing may result in a higher density of low-spin levels predicted below 1.5 MeV.

The systematics of the negative-parity levels in the $N=88$ isotones around [147]Pr are shown in Fig. 8, along with the levels in the even-even core nuclei. With an increase in proton number from [149]Pm to [151]Eu, the posi-

tion of the $11/2^-$ state, which is the bandhead of the $K=1/2^-$ band, decreases as expected with the rise in the proton Fermi surface towards midshell. The presence of the low-energy $3/2^-$ and $5/2^-$ states in [149]Pm, which are proposed [38] to have properties separate from the other negative-parity levels in this energy region, and the presence of the negative-parity level at 238 keV in [145]La, suggest that a more complex configuration mixing, possibly involving the low-energy octupole states in the even-even core nuclei, may manifest itself at low energy in these $N=88$ isotones.

The PTRM code used here, however, does not include provisions for the mixing of positive- and negative-parity states, as the octupole (β_3) degree of freedom is excluded from the calculations. Therefore, if these low-energy low-spin negative-parity states arise from complex configuration mixing involving β_3 deformation, these levels would lie outside the PTRM model space.

Another aspect of the drop in position of the negative-parity levels as N increases toward 90 can be obtained from the proton pickup reactions on Sm nuclides. Lee et al. [39] studied the $(d, ^3He)$ reactions on the Sm nuclides and demonstrated the sharp rise in pickup strength for the $h_{11/2}$ $l=5$ orbital as N crossed 90. While this process is rather sharp in the even-mass nuclides, it can
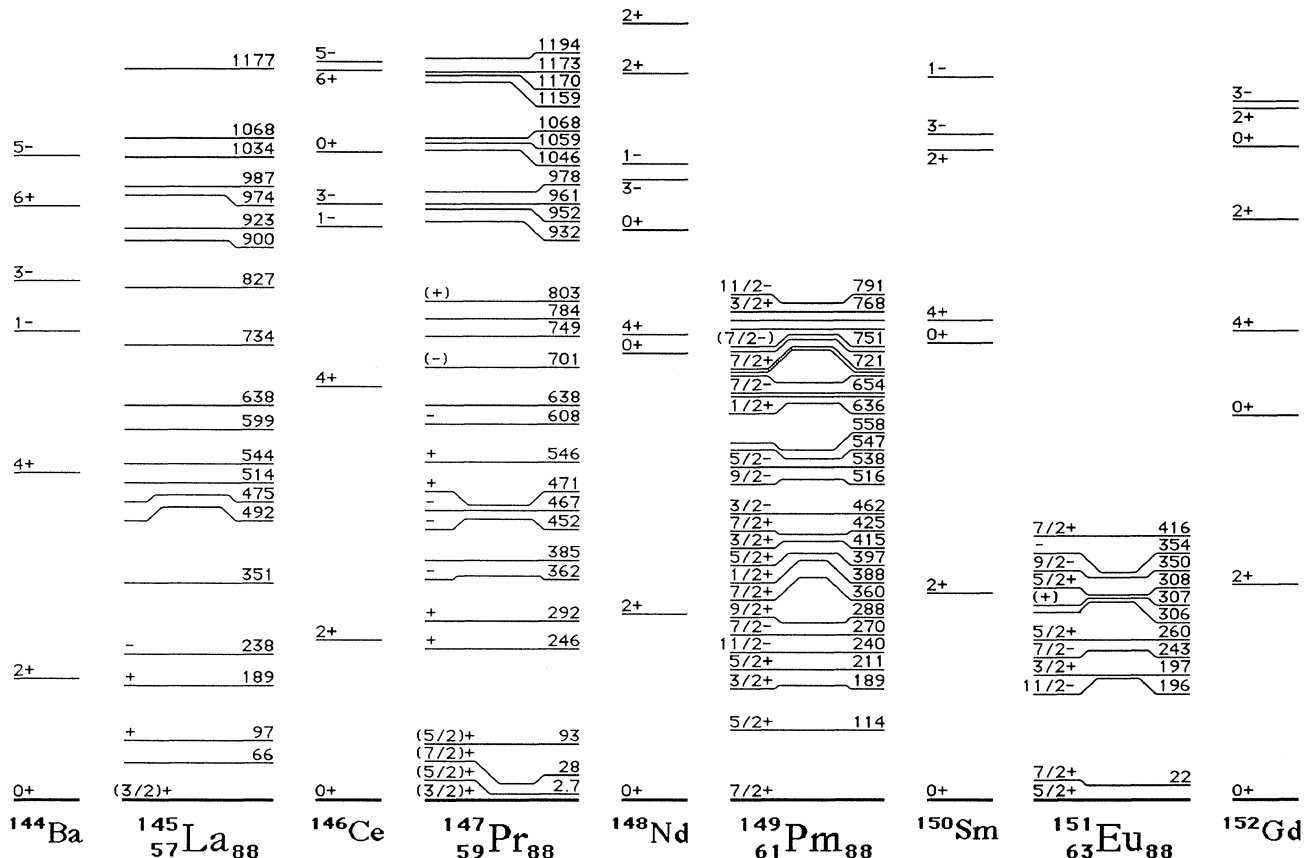
FIG. 8. Systematics of the $N=88$ isotones. The even-even core nuclei are also shown to better illustrate the drop in the energy of the 1^- and 3^- states in these nuclei.

be seen to be more gradual in the odd-mass nuclides resulting in the appearance of parity-dependent shape coexistence in these nuclides. Namely, the nuclides with $N < 90$ show both low-energy $h_{11/2}$ levels that have low occupancy and relatively spherical shape similar to that described above for the positive-parity levels. These coexist with the more deformed Nilsson low-spin negative-parity orbitals that arise from the transfer of additional protons into the $h_{11/2}$ orbitals, an interaction doubtless strengthened by the increasing occupancy of the spin-orbit partner neutron $h_{9/2}$ orbitals as N approaches 90.

C. Deep proton-hole states and the one-proton transfer reaction

In a study [40] of inner proton-hole states, Zybert et al. used the ^{148}Nd(t,α) single-proton transfer reaction to measure the $l=4$ strength at high excitation energies in ^{147}Pr. Their interpretation of the peaks in the low excitation part of the ^{148}Nd$(t,\alpha)^{147}$Pr reaction, however, has been made with the assumption that the peak appearing at the lowest excitation energy corresponds with the ground state of ^{147}Pr. We propose this is not the case, and that this peak, which is reported by Zybert et al. to have an angular distribution pattern characteristic of $l=4$ angular momentum transfer, actually corresponds to the level at 28 keV above the ground state in ^{147}Pr. Instead, we suggest that the 60-keV gap they indicate between the first two excited states is the gap between the levels we propose at 28 and 93 keV.

The excitation energies given for the transfer peaks observed from the ^{148}Nd(t,α) reaction are, therefore, relative to the second excited state in ^{147}Pr, and the absolute energy for each peak is the excitation energy plus 28 keV. The resulting agreement of the absolute transfer peak energies with the low-energy structure of ^{147}Pr reported here is very good, within their error limits of ± 20 keV. The peak in the transfer spectrum having an angular distribution characteristic of $l=5$ momentum transfer would now correspond to a level near 380 keV in ^{147}Pr, and suggests that the $11/2^-$ level that retains the bulk of the single-particle transfer strength lies nearly degenerate with the low-spin negative-parity level we have established at 362 keV.

The appearance of three states, which lie less than 100 keV above the ground state, in ^{147}Pr suggests that the quadrupole deformation is somewhat larger than the $\beta_2 = 0.04$ proposed by Zybert et al. for this nucleus, and

that the predictions of the TRS calculations discussed above are much more in line with the actual value. A quadrupole deformation of $\beta_2 = 0.17$ results in severe crossings of the branches of the $g_{9/2}$ and $g_{7/2}$ subshells, which clouds the interpretation that the bump in the one-proton transfer reaction corresponding to $l=4$ momentum transfer can be attributed solely to the orbital belonging to the $g_{9/2}$ subshell. Therefore, the differences in the "bumps" that appear at high excitation energy in the proton transfer reactions for ^{147}Pr, ^{151}Pm, and ^{155}Eu may not be a sole manifestation of simple nuclear shell effects.

VI. CONCLUSION

We have studied the level structure of ^{147}Pr fed in the β^- decay of ^{147}Ce. The proposed level scheme includes a high level density below 100 keV and several negative-parity states, which lie a very low excitation energy. Using the particle-plus-triaxial rotor model, we have calculated the negative- and positive-parity level structures for ^{145,147,149}Pr. The experimental positive-parity level density below 1 MeV is reproduced well by the PTRM calculations, and supports the shape predictions ($\beta_2 = 0.17$, $\gamma = 0°$) of the total Routhian surface calculations. Without the inclusion of Coriolis attenuation, the PTRM calculations predict a lower negative-parity level density for low-spin states below 1.5 MeV than what is observed experimentally for ^{145,147}Pr, suggesting a possible role for octupole degrees of freedom in the low-energy level structure for these Pr nuclides.

ACKNOWLEDGMENTS

[1] W. McLatchie, J. E. Kitching, and W. Darcey, Phys. Lett. 30B, 529 (1969).

[2] A. Passoja, J. Kantele, M. Luontama, R. Julin, E. Hammaren, P. O. Lipas, and P. Toivonen, J. Phys. G 12, 1047 (1986).

[3] J. L. Wood, K. Heyde, W. Nazarewicz, M. Huyse, and P. van Duppen, Phys. Rep. 215, 101 (1992).

[4] H. Mach, M. Hellström, B. Fogelberg, D. Jerrestam, and L. Spanier, Phys. Rev. C 46, 1849 (1992).

[5] W. R. Phillips, I. Ahmad, H. Emling, R. Holtzman, R. V.

F. Janssens, T. L. Khoo, and M. W. Drigert, Phys. Rev. Lett. 57, 3257 (1986).

[6] W. R. Phillips, R. V. F. Janssens, I. Ahmad, H. Emling, R. Holtzman, T. L. Khoo, and M. W. Drigert, Phys. Lett. B 212, 402 (1988).

[7] W. Urban, R. M. Lieder, W. Gast, G. Hebbinghaus, A. Kramer-Flecken, T. Morek, T. Rzaca-Urban, W. Nazarewicz, and S. L. Tabor, Phys. Lett. B 200, 424 (1988).

[8] E. Hammaren, E. Liukkonen, M. Piiparinen, J. Kownacki, Z. Sujkowski, Th. Lindblad, and H. Ryde, Nucl. Phys.

A321, 71 (1979).

[9] W. Urban, R. M. Lider, W. Gast, G. Hebbinghaus, A. Kramer-Flecken, K. P. Blume, and H. Hubel, Phys. Lett. B 185, 337 (1987).

[10] G. A. Leander, W. Nazarewicz, P. Olanders, I. Ragnarsson, and J. Dudek, Phys. Lett. 152B, 284 (1985).

[11] J. D. Robertson, S. H. Faller, W. B. Walters, R. L. Gill, H. Mach, A. Piotrowski, E. F. Zganjar, H. Dejbakhsh, and R. F. Petry, Phys. Rev. C 34, 1012 (1986).

[12] J. D. Robertson, P. F. Mantica, Jr., S. H. Faller, C. A. Stone, E. M. Baum, and W. B. Walters, Phys. Rev. C 40, 2804 (1989).

[13] D. F. Kusnezov, D. R. Nethaway, and R. A. Meyer, Phys. Rev. C 40, 924 (1989).

[14] E. M. Baum, J. D. Robertson, P. F. Mantica, Jr., S. H. Faller, C. A. Stone, W. B. Walters, R. A. Meyer, and D. F. Kusnezov, Phys. Rev. C 39, 1514 (1989).

[15] O. Scholten and N. Blasi, Nucl. Phys. A380, 509 (1982).

[16] O. Scholten and T. Ozzello, Nucl. Phys. A424, 22 (1984).

[17] F. Schussler, B. Pfeiffer, H. Lawin, E. Monnand, J. Munzel, J. A. Pinston, and K. Sistemisch, in *Proceedings of the 4th International Conference on Nuclei Far From Stability,* edited by P. G. Hansen and O. B. Neilsen (Skolen, Helsingor, 1981), p. 589.

[18] M. Totsuka, S. Fujita, K. Mio, K. Kawade, H. Yamamoto, T. Katoh, and T. Nagahara, J. Nucl. Sci. Technol. 19, 765 (1982).

[19] J. A. Pinston, R. Roussille, G. Bailleu, J. Blachot, J. P. Bocquet, E. Monnand, B. Pfeiffer, H. Schrader, and F. Schussler, Nucl. Phys. A246, 395 (1975).

[20] P. F. Mantica, Jr., E. F. Baum, J. D. Robertson, C. A. Stone, W. B. Walters, D. F. Kusnezov, and R. A. Meyer, in *Proceedings of the 5th International Conference on Nuclei Far From Stability,* edited by I. S. Towner, AIP Conf. Proc. No. 164 (AIP, New York, 1988), p. 455.

[21] R. L. Gill, M. L. Stelts, R. E. Chrien, V. Manzella, H. I. Liou, and S. Shostak, Nucl. Instrum. Methods 186, 243 (1981).

[22] R. L. Gill and A. Piotrowski, Nucl. Instrum. Methods A 234, 213 (1985).

[23] A. Piotrowski, R. L. Gill, and D. C. McDonald, Nucl. Instrum. Methods A 224, 1 (1984).

[24] See AIP document No. PAPS PRVCA-48-1579-17 for 17 pages of tables. Order by PAPS number and journal reference from the American Institute of Physics, Physics Auxiliary Publication Service, 500 Sunnyside Blvd., Woodbury, N.Y. 11797-2999. The prepaid price is $1.50 for each microfiche (60 pages) and $5.00 for photocopies of up to 30 pages and $0.15 for each additional page over 30 pages. Airmail additional. Make checks payable to the American Institute of Physics.

[25] E. der Mateosian and L. K. Peker, Nucl. Data Sheets 66, 705 (1992).

[26] F. Rösel, H. M. Fries, K. Alder, and H. C. Pauli, At. Data Nucl. Data Tables 21, 293 (1978).

[27] H. Yamamoto, Y. Ikeda, K. Kawade, T. Katoh, and T. Nagahara, J. Inorg. Nucl. Chem. 43, 855 (1981).

[28] S. E. Larsson, G. A. Leander, and I. Ragnarsson, Nucl. Phys. A307, 189 (1978).

[29] I. Ragnarsson and P. Semmes, Hyperfine Interactions 43, 425 (1988).

[30] W. Nazarewicz, J. Dudek, R. Bengtsson, T. Bengtsson, and I. Ragnarsson, Nucl. Phys. A435, 397 (1985).

[31] S. Cwiok, J. Dudek, W. Nazarewicz, J. Skalski, and T. Werner, Comput. Phys. Commun. 46, 379 (1987).

[32] W. Nazarewicz, R. Wyss, and A. Johnson, Nucl. Phys. A503, 285 (1989).

[33] T. Glasmacher, D. D. Caussyn, P. D. Cottle, T. D. Johnson, K. W. Kemper, and P. C. Womble, Phys. Rev. C 45, 1619 (1992).

[34] J. Dudek, A. Majhofer, and J. Skalski, J. Phys. G 6, 447 (1980).

[35] P. Semmes, *The Particle + Triaxial Rotor Model: A Users Guide* (1991).

[36] H.-Q. Jin, L. L. Riedinger, C.-H. Yu, W. Nazarewicz, R. Wyss, J.-Y. Zhang, C. Baktash, J. Garrett, N. Johnson, I. Lee, and F. McGowan, Phys. Lett. B 277, 387 (1992).

[37] J. Almberger, I. Hammamoto, and G. Leander, Phys. Scr. 22, 33 (1980).

[38] W. B. Walters, M. D. Glascock, E. W. Schneider, R. A. Meyer, H. A. Smith, Jr., and M. E. Bunker, *Nuclear Structure of Fission Products* (Institute of Physics, Bristol, 1980), p. 303.

[39] I. S. Lee, W. J. Jordan, J. V. Maher, R. Kamermans, J. W. Smits, and R. H. Siemssen, Nucl. Phys. A371, 111 (1981).

[40] L. Zybert, J. B. A. England, G. M. Field, O. Karban, R. Zybert, M. Becha, C. N. Pinder, G. C. Morrison, M. Bentley, P. Fallon, R. Moktah, J. W. Roberts, and J. F. Sharpey-Schafer, Nucl. Phys. A510, 441 (1990).